Electronic Supplementary Material (ESI) for Inorganic Chemistry Frontiers.

Supporting Information

Multidimensional In_2S_3-$CuInS_2$ Heterostructure for Photocatalytic Carbon Dioxide Reduction

Jinman Yang[a], Xingwang Zhu[a], Zhao Mo[a], Jianjian Yi[a], Jia Yan[a], Jiujun Deng[a], Yuanguo Xu[a], Yuanbin She[b], Junchao Qian[c], Hui Xu[a,*], Huaming Li[a,*]

[a.]School of Chemistry and Chemical Engineering, Institute for Energy Research, Jiangsu University, Zhenjiang, 212013, P.R. China

[b.]State Key Laboratory Breeding Base of Green Chemistry-Synthesis Technology, College of Chemical Engineering, Zhejiang University of Technology, Hangzhou, 310014, China

[c.]School of Chemistry, Biology and Materials Engineering, Suzhou University of Science and Technology, Suzhou, 215009, China

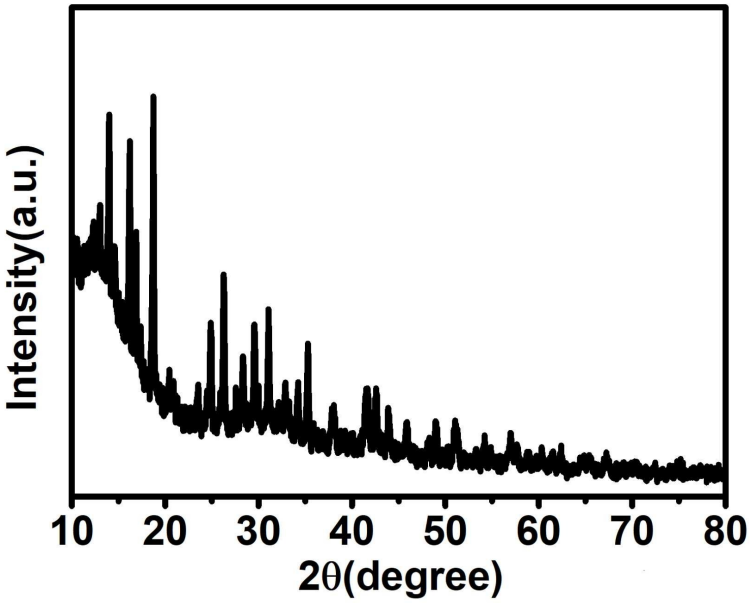

Figure S1. XRD pattern of MIL-68.

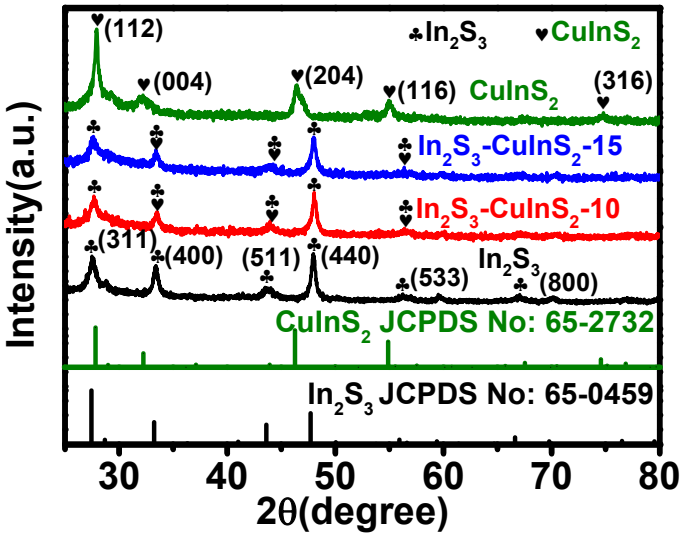

Figure S2. Standard XRD patterns of standard In_2S_3 and $CuInS_2$, XRD patterns of In_2S_3, In_2S_3-$CuInS_2$-10, In_2S_3-$CuInS_2$-15 and $CuInS_2$.

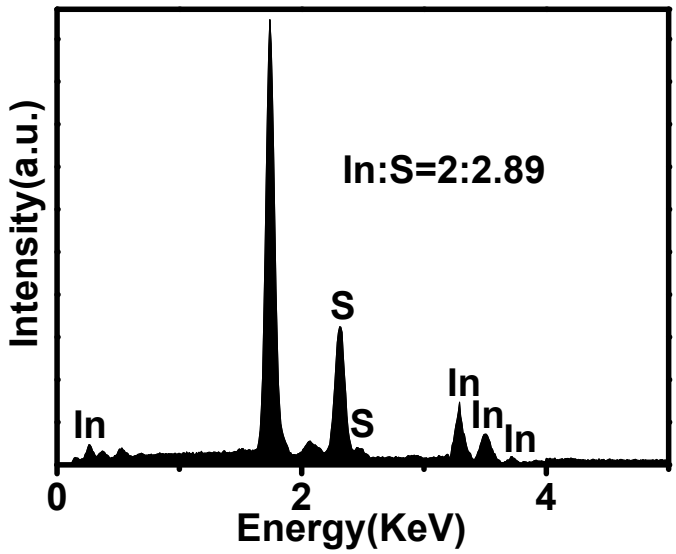

Figure S3. EDX spectrum In_2S_3.

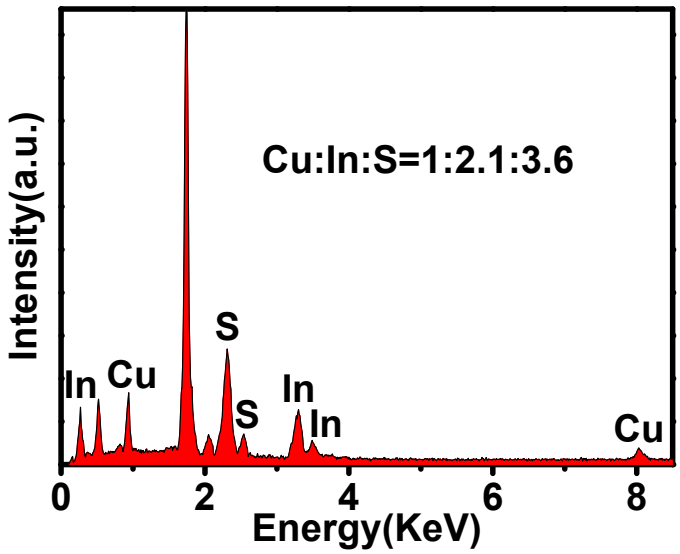

Figure S4. EDX spectrum of In_2S_3-$CuInS_2$-10.

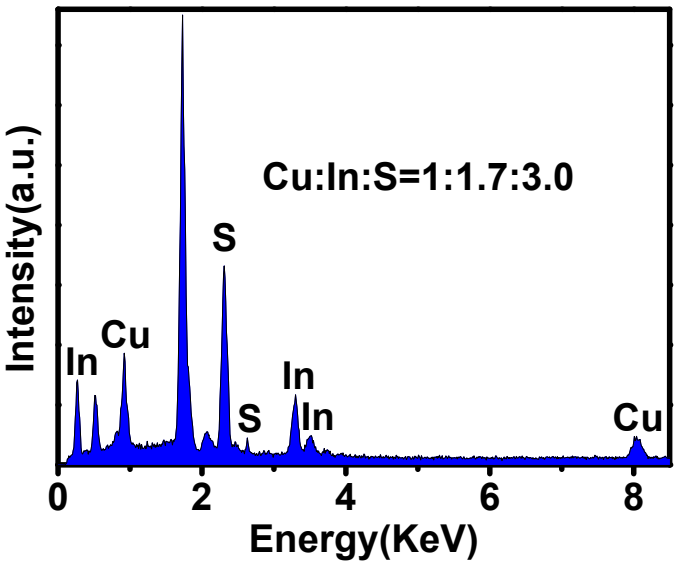

Figure S5. EDX spectrum of In_2S_3-$CuInS_2$-15.

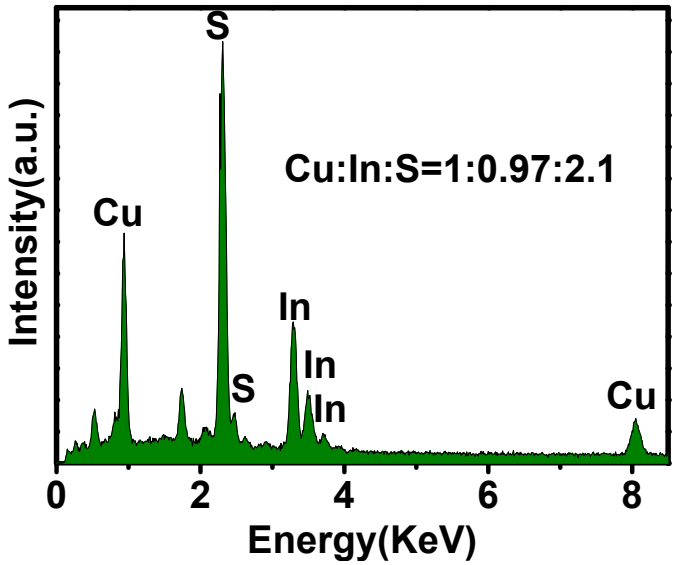

Figure S6. EDX spectrum of $CuInS_2$.

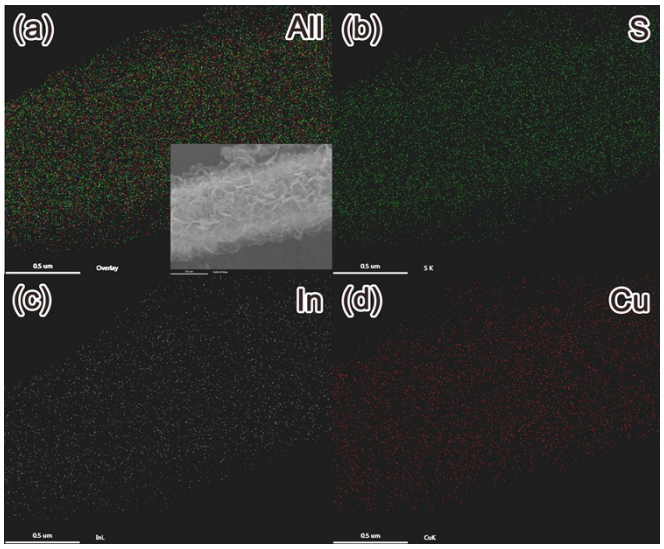

Figure S7. Elemental mapping images of In_2S_3-$CuInS_2$-15.

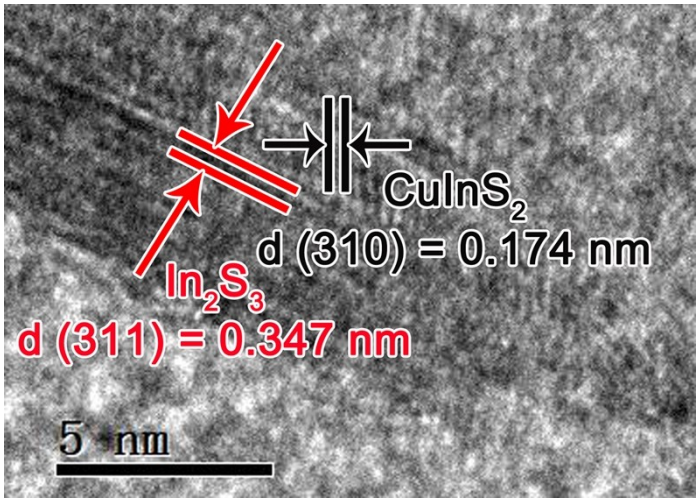

Figure S8. High-resolution TEM image of In_2S_3-$CuInS_2$-15.

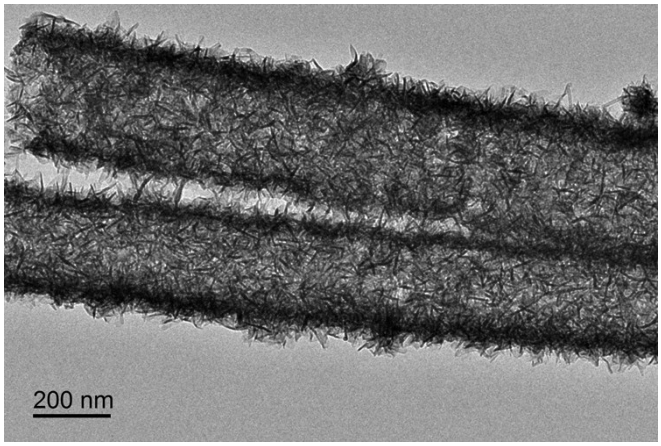

Figure S9. TEM image of In_2S_3-$CuInS_2$-10.

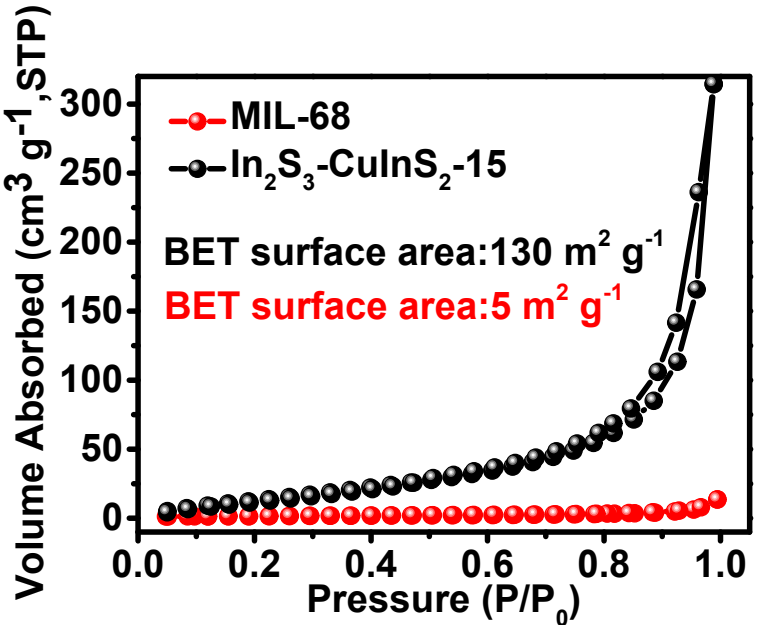

Figure S10. N_2 adsorption-desorption isotherms of MIL-68 and In_2S_3-$CuInS_2$-15.

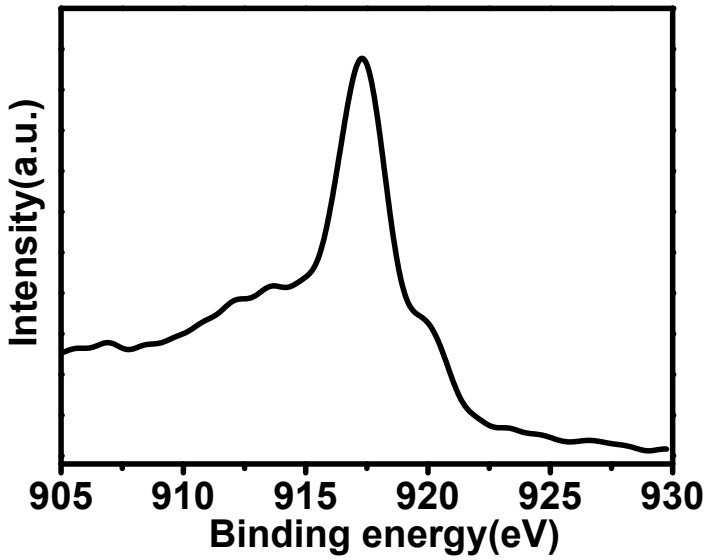

Figure S11. The Auger electron spectroscopy of Cu.

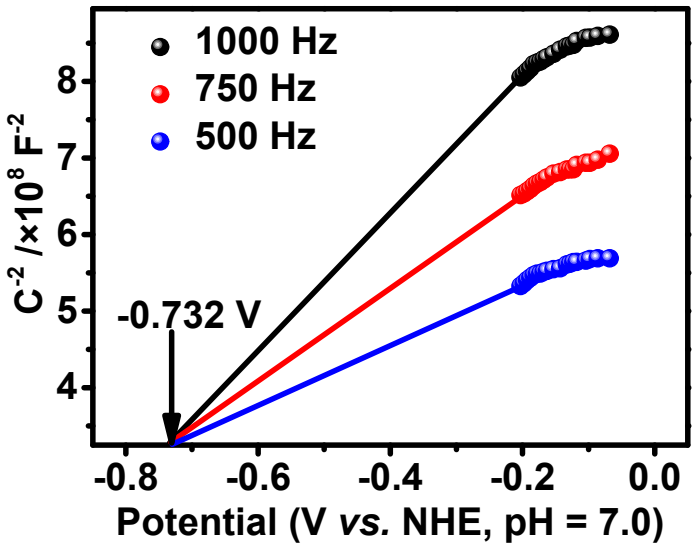

Figure S12. Mott-Schottky plots of pure In_2S_3.

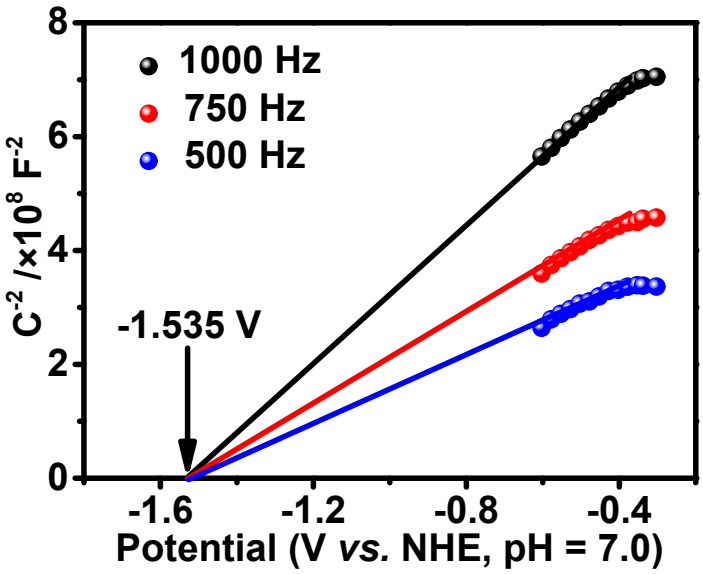

Figure S13. Mott-Schottky plots of pure $CuInS_2$.

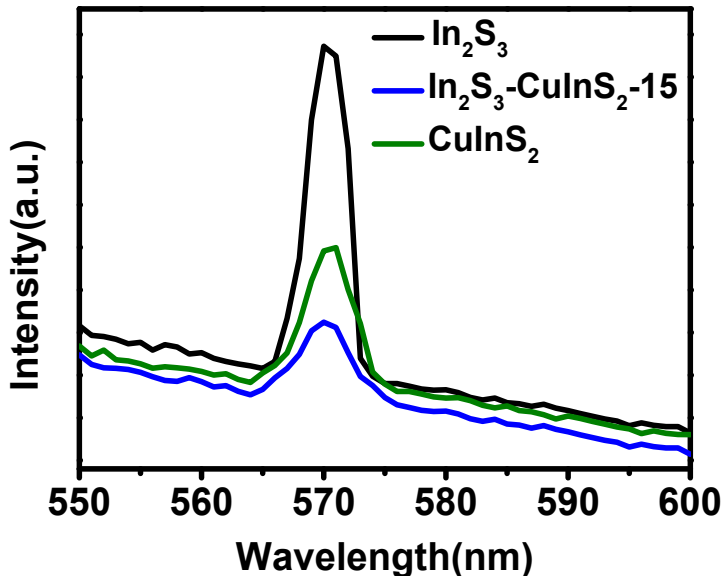

Figure S14. Photoluminescence emission spectras of In_2S_3, In_2S_3-$CuInS_2$-15 and $CuInS_2$.

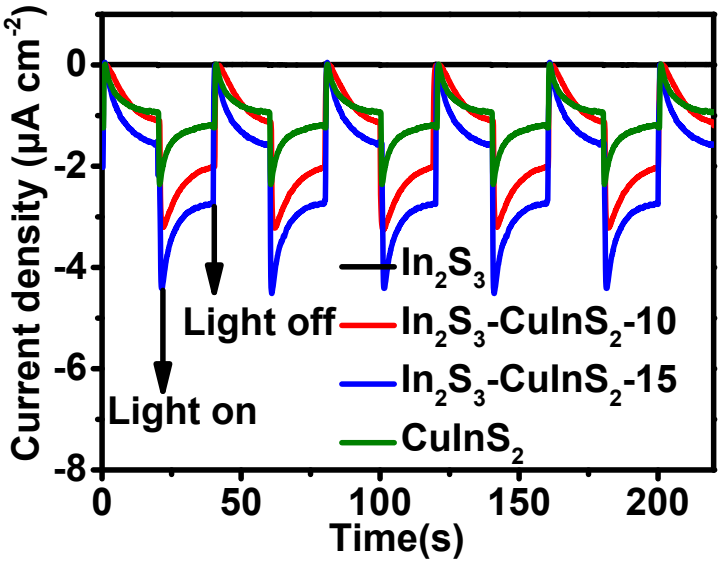

Figure S15. The transient photocurrent responses of In_2S_3, In_2S_3-$CuInS_2$-10, In_2S_3-$CuInS_2$-15 and $CuInS_2$.

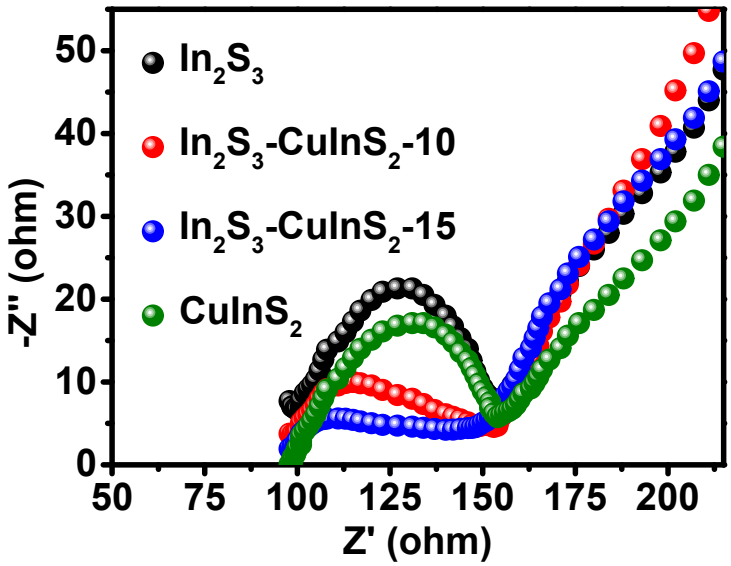

Figure S16. Electrochemical impedance spectroscopy (EIS) plots of In_2S_3, In_2S_3-$CuInS_2$-10, In_2S_3-$CuInS_2$-15 and $CuInS_2$.

Table S1. Comparison of the CO_2 photoreduction performance of In_2S_3-$CuInS_2$-15 catalyst with other catalysts.

Light source	Catalyst	Experimental conductions	Experimental conduction μmol g^{-1} h^{-1}	Reference
300 W Xe lamp	**In_2S_3-$CuInS_2$**	**$CoCl_2$, 2,2-bipyridine, TEOA, MeCN**	**CO: 19**	**This work**
300 W Xe lamp	$NiCo_2O_4$	TEOA, MeCN	CO: 7	1
300 W Xe lamp	g-C_3N_4	$CoCl_2$, 2,2-bipyridine, TEOA, MeCN	CO: 6	2
450 W Xe lamp	Cu_2S/Pt	TEOA	CO: 3.02 CH_4: 1.03	3
500 W Xe lamp	Ni (0.2 mol%) doped ZnS	TEOA, MeCN	CO: 1.67 HCOOH: 0.67	4
500 W Xe lamp	NH_2-MIL-125(Ti)	TEOA, MeCN	HCOOH: 16	5
500 W Xe lamp	NH_2-Uio-66(Zr)	TEOA, MeCN	HCOOH: 26.4	6
300 W Xe lamp	UiO-66/CNNS	TEOA, MeCN	CO: 9.79	7
300 W Xe lamp	Co-porphyrin/carbon nitride	TEOA, MeCN	CO: 17	8

References

[1] Z. Wang, M. Jiang, J. Qin, H. Zhou, Z. Ding, *Phys. Chem. Chem. Phys*., 2015, **17**, 16040-16046.

[2] J. Lin, Z. Pan, X. Wang, *ACS Sustainable Chem. Eng.,* 2014, **2**, 353-358.

[3] A. Manzi, T. Simon, C. Sonnleitner, M. Doblinger, R. Wyrwich, O. Stern, J. Stolarczyk, J. Feldmann, *J. Am. Chem. Soc.* 2015, **137**, 14007-14010.

[4] T. M. Suzuki, T. Takayama, S. Sato, A. Iwase, A. Kudo, T. Morikawa, *Appl. Catal. B: Environ.* 2018, **224**, 572-578.

[5] D. Sun, Y. Fu, W. Liu, L. Ye, D. Wang, L. Yang, X. Fu, Z. Li, *Chem. Eur. J.* 2013, **19**, 14279-14285.

[6] Y. Fu, D. Sun, Y. Chen, R. Huang, Z. Ding, X. Fu, Z. Li, *Angew. Chem. Int. Ed.*, 2012, **51**, 3364-3367.

[7] L. Shi, T. Wang, H. Zhang, K. Chang, J. Ye, *Adv. Funct. Mater.,* 2015, **25**, 5360-5367.

[8] G. Zhao, H. Pang, G. Liu, P. Li, H. Liu, H. Zhang, L. Shi, J. Ye, *Appl. Catal. B: Environ.,* 2017, **200**, 141-149.